 AFRL-PR-ED-TR-2003-0030

Advanced Rocket Propulsion Technologies Boron Vapor Source for HEDM

Paul C. Nordine

Containerless Research Inc.
906 University Place
Evanston IL 60201-3149

June 2003

SBIR Phase I Final Report

AIR FORCE RESEARCH LABORATORY
AIR FORCE MATERIEL COMMAND
EDWARDS AIR FORCE BASE CA 93524-7048

REPORT DOCUMENTATION PAGE

Form Approved
OMB No. 0704-0188

1. REPORT DATE *(DD-MM-YYYY)*	**2. REPORT TYPE**	**3. DATES COVERED** *(From - To)*
10-06-2003	SBIR Phase I Final	24 May 2001 – 26 April 2002

4. TITLE AND SUBTITLE

Advanced Rocket Propulsion Technologies Boron Vapor Source for HEDM

5a. CONTRACT NUMBER
F04611-01-C-0034

5b. GRANT NUMBER

5c. PROGRAM ELEMENT NUMBER
65502F

6. AUTHOR(S)
Paul C. Nordine

5d. PROJECT NUMBER
3005

5e. TASK NUMBER
01VS

5f. WORK UNIT NUMBER
549883

7. PERFORMING ORGANIZATION NAME(S) AND ADDRESS(ES)

Containerless Research Inc.
906 University Place
Evanston IL 60201-3149

8. PERFORMING ORGANIZATION REPORT NO.

CRI 31-0004F

9. SPONSORING / MONITORING AGENCY NAME(S) AND ADDRESS(ES)

Air Force Research Laboratory (AFMC)
AFRL/PRSP
10 East Saturn Blvd.
Edwards AFB CA 93524-7680

10. SPONSOR/MONITOR'S ACRONYM(S)

11. SPONSOR/MONITOR'S REPORT NUMBER(S)
AFRL-PR-ED-TR-2003-0030

12. DISTRIBUTION / AVAILABILITY STATEMENT
Approved for public release; distribution unlimited.

13. SUPPLEMENTARY NOTES

14. ABSTRACT

Report developed under SBIR contract for topic AF01 -190.

The research reported here is directed to the development of a boron vapor source for application in HEDM research. Specific goals of the research were (i) a boron vapor flux that allows formation of transparent solid pH2 with high concentrations of boron dopant species, up to 5 molar %, (ii) a design for integration with the cryo-solid spectroscopy equipment at AFRL/PRSP, Edwards Air Force Base.

The boron vapor source was fabricated and tested. Its performance was demonstrated to agree well with the diffuse free evaporation model. C02 laser beam heating and melting of the boron samples was shown to yield intrinsic control of the boron sample temperature at the melting point, and a well-controlled boron flux. The boron vapor flux obtained with the apparatus is sufficient to prepare boron-doped pH2 HEDM solids at rates of 100 micrometers/hour at boron concentrations of 1.4 mol %, and at much higher rates at smaller boron concentrations. A Phase II SBIR proposal was prepared and submitted to the Air Force.

15. SUBJECT TERMS
SBIR; boron vapor; HEDM

16. SECURITY CLASSIFICATION OF:			**17. LIMITATION OF ABSTRACT**	**18. NUMBER OF PAGES**	**19a. NAME OF RESPONSIBLE PERSON**
					Carl W. Larson
a. REPORT	**b. ABSTRACT**	**c. THIS PAGE**	A	33	**19b. TELEPHONE NO** *(include area code)*
Unclassified	**Unclassified**	**Unclassified**			(661) 275-6104

Standard Form 298 (Rev. 8-98)
Prescribed by ANSI Std. 239.18

FOREWORD

This Final Technical Report presents the results of a Phase I SBIR study performed by Containerless Research Inc., Evanston, IL, under Contract No. F04611-01-C-0034, for the Air Force Research Laboratory (AFRL), Edwards AFB, CA. The Project Manager for AFRL was Dr. C. W. (Bill) Larson.

This report has been reviewed and is approved for release and distribution in accordance with the distribution statement on the cover and on the SF Form 298. This report is published in the interest of scientific and technical information exchange and does not constitute approval or disapproval of its ideas or findings.

CARL W. LARSON
Project Manager

WAYNE M. KALLIOMAA
Acting Chief, Propellants Branch

PHILIP A. KESSEL
Technical Advisor, Space and Missile Propulsion Division

RANNEY G. ADAMS III
Director
Public Affairs

AFRL PAS 03-116

This Page Intentionally Left Blank

TABLE OF CONTENTS

LIST OF FIGURES

LIST OF TABLES

GLOSSARY

Ar	Argon gas
B	Boron
BO	boron oxide vapor
CO	carbon monoxide vapor
CO_2	Carbon dioxide
HEDM	High energy density material
NaCl	Sodium chloride
O_2	Oxygen gas
pH_2	Para hydrogen
ppm	parts per million
sccm	Standard cubic cm^3 per minute (flow of gas in units of cm3 at standard conditions of 1 atm pressure and 0°C temperature)
ZnSe	Zinc selenide

This Page Intentionally Left Blank

1.0 INTRODUCTION

This report describes results from a Phase I SBIR research contract directed to the development of a boron vapor source for application to HEDM. The HEDM of special interest is a mixture of solid pH_2 and atomic boron, formed by co-deposition of boron vapor and gaseous pH_2 on a cold surface. This material, at boron concentration levels of approximately 5 mole %, is a monopropellant with the potential to yield a specific impulse significantly greater than conventional rocket propellants, at greatly reduced propellant and rocket engine temperatures.

The project has two primary goals directed to Air Force objectives. The first goal is to achieve a boron vapor flux that allows formation of transparent solid pH_2 with high concentrations of boron dopant species, up to 5 molar %. The second goal is a boron vapor source design for integration with the cryo-solid spectroscopy equipment at AFRL/PRSP, Edwards Air Force Base, and use in HEDM research. These goals were met in the research.

2.0 TECHNICAL RESULTS

2.1 Boron Deposition Apparatus

Figure 1 illustrates the boron vapor source design. The apparatus is constructed from stainless steel vacuum hardware, with copper gaskets to seal flanges, except at O-ring connections for a ZnSe window for the CO_2 laser heating beam and a glass window for observation and optical pyrometry.

The liquid boron is formed by laser melting of a boron sample on a water-cooled hearth supported at the bottom of the vacuum chamber on flange 3. The hearth may also be used for sample preparation. Vapor from the liquid boron flows to the deposition chamber, which is shown in the design drawing as the octagonal chamber that is used for spectroscopy at AFRL, item 4 in the drawing. Shutters (item 13) prevent flow of boron onto the pyrometer window at flange 19 (except during temperature measurements) and to the deposition region as needed.

In the Phase I research, a film thickness rate monitor was installed where the deposition chamber is shown in Figure 1, and the shutter to the deposition chamber was replaced with a shutter included in the rate monitor device. The rate monitor is Model STM-100 from Sycon Instruments, Inc.

Laser beam heating is from above, through a ZnSe window at flange 16. The heating laser beam passes through a section that includes a special method to protect the ZnSe window from deposition of boron vapor. The stainless steel cross has a linear motion feedthrough (item 7) that holds a thin NaCl window. The inexpensive NaCl window is held in the heating laser beam to prevent boron vapor from reaching the ZnSe vacuum window. The laser beam is focussed to a pinhole below the NaCl window that is designed so that boron will deposit only on a small spot on the window. The linear motion feedthrough translates the NaCl window during the experiment to keep a clear path for the heating laser beam. After a period of time, the window may be cleaned, or replaced for subsequent experiments.

REPORT DOCUMENTATION PAGE

Form Approved OMB No. 0704-0188

1. REPORT DATE (DD-MM-YYYY)	2. REPORT TYPE	3. DATES COVERED (FROM - TO)
10-06-2003	SBIR Phase I Final	24-05-2001 to 26-04-2002

4. TITLE AND SUBTITLE
Advanced Rocket Propulsion Technologies Boron Vapor Source for HEDM
Unclassified

5a. CONTRACT NUMBER
F04611-01-C-0034

5b. GRANT NUMBER

5c. PROGRAM ELEMENT NUMBER
65502F

6. AUTHOR(S)
Nordine, Paul C. ;

5d. PROJECT NUMBER
3005

5e. TASK NUMBER
01VS

5f. WORK UNIT NUMBER

7. PERFORMING ORGANIZATION NAME AND ADDRESS
Containerless Research Inc.
906 University Place
Evanston, IL60201-3149

8. PERFORMING ORGANIZATION REPORT NUMBER
CRI 31-0004F

9. SPONSORING/MONITORING AGENCY NAME AND ADDRESS
Air Force Research Laboratory (AFMC)
AFRL/PRSP
10 E. Saturn Blvd.
Edwards AFB, CA93524-7680

10. SPONSOR/MONITOR'S ACRONYM(S)

11. SPONSOR/MONITOR'S REPORT NUMBER(S)
AFRL-PR-ED-TR-2003-0030

12. DISTRIBUTION/AVAILABILITY STATEMENT
APUBLIC RELEASE
,

13. SUPPLEMENTARY NOTES

14. ABSTRACT
Report developed under SBIR contract for topic AF01 -190. The research reported here is directed to the development of a boron vapor source for application in HEDM research. Specific goals of the research were (i) a boron vapor flux that allows formation of transparent solid pH2 with high concentrations of boron dopant species, up to 5 molar %, (ii) a design for integration with the cryo-solid spectroscopy equipment at AFRL/PRSP, Edwards Air Force Base. The boron vapor source was fabricated and tested. Its performance was demonstrated to agree well with the diffuse free evaporation model. C02 laser beam heating and melting of the boron samples was shown to yield intrinsic control of the boron sample temperature at the melting point, and a well-controlled boron flux. The boron vapor flux obtained with the apparatus is sufficient to prepare boron-doped pH2 HEDM solids at rates of 100 micrometers/hour at boron concentrations of 1.4 mol %, and at much higher rates at smaller boron concentrations. A Phase II SBIR proposal was prepared and submitted to the Air Force.

15. SUBJECT TERMS
SBIR; boron vapor; HEDM

16. SECURITY CLASSIFICATION OF:			17. LIMITATION OF ABSTRACT	18. NUMBER OF PAGES	19. NAME OF RESPONSIBLE PERSON
a. REPORT	b. ABSTRACT	c. THIS PAGE	Same as Report (SAR)	33	Larson, Carl W. Carl.Larson@edwards.af.mil
Unclassified	Unclassified	Unclassified			19b. TELEPHONE NUMBER International Area Code Area Code Telephone Number 661275-6104 DSN 525-6104

The vacuum system includes a turbomolecular pump to obtain high vacuum. This pump is rated to achieve a high compression ratio for hydrogen. The plan and elevation views of the boron vapor source (not given here) show that this system will fit in the available space at the AFRL spectroscopy facility.

As drawn, the distance from the boron vapor source to the substrate for spectroscopy experiments is 6" (15 cm). Table 1 gives the deposition rates, assuming a 6 mm diameter boron vapor source located 15 cm from the deposition target and for the source temperatures and HEDM concentrations given in the table.

Table 1 Deposition Rate of B/pH_2 HEDM for a 6 mm Diameter Boron Vapor Source Located 15 cm from the Deposition Target

	B-Source conditions		Deposition rate of HEDM, μm/hr		
T, K	P, Torr	Equilibrium flux, cm^{-2} s^{-1}	0.1% B	1% B	5% B
2360	9.88×10^{-3}	2.17×10^{18}	600	60	12
2410	1.73×10^{-2}	3.77×10^{18}	1050	105	21

The deposition rate is calculated from the vapor pressure of boron at the given temperature and the concentration assumed for boron atoms in the B/pH_2 HEDM. For purposes of this calculation the total molar volume of the HEDM solid was taken equal to that of pH_2, 23.2 cm^3/mol.

Some further details of the apparatus are illustrated in Figure 2. The figure shows a side, partially cut-away view of the system. Figure 3 is a photograph of the boron vapor source apparatus. The photograph shows 45° angled ports for temperature measurement (left) observation (center) and the boron deposition monitor (right). A Bayard Alpert ion gage is connected to the deposition monitor structure and a 70 l/s turbomolecular pump is at the back.

Nearly spherical, approximately 3 mm diameter samples were used in some experiments. Larger diameter flattened samples were made by melting several small samples together and used in other experiments. The larger flattened samples could be mounted with their surface at 45º to the incident heating laser beam direction, i.e., normal to either the pyrometer viewing direction or to the direction of the deposition monitor. A spectral radiation pyrometer with effective wavelength equal to 650 nm was used in the experiments.

A "blast shield" surrounds the boron sample. Its purpose is to prevent boron vapor deposition throughout the apparatus, except where boron can flow through openings in the blast shield. The openings are for the laser beam heating, viewing, pyrometry, and towards the deposition monitor. Two blast shields were used in the experiments. The first blast shield was machined from aluminum, which served to absorb a substantial fraction of the CO_2 laser beam energy reflected from the boron sample. (The oxide coating on aluminum is a very good absorber at the 10.6 μm laser wavelength.) Heating of the aluminum blast shield was sufficient that it deformed after several experiments. The second blast shield was machined from steel, and did not deform from heating by reflected laser energy.

The surface of the deposition rate monitor at which the boron vapor flux was measured is located 22.7 cm from the nominal boron sample position. The apparatus was first operated without any apertures in the tube leading to the rate monitor. Later, baffles were added at the locations indicated in Figure 2, to reduce the transmission of incandescent radiation and reflected laser radiation to the deposition monitor. The baffles are circular apertures that stop most of the radiation reflected from the tube walls while maintaining an open line of sight between the boron sample surface and the surface of the rate sensor.

2.2 Synthesis of Pure Boron

The boron samples used to supply a flux of pure boron vapor were prepared by arc- or laser hearth-melting to form dense spheroids, followed by purification under containerless conditions to remove residual oxygen, nitrogen, and carbon.

Eagle Picher boron, Lot No. F872-1298 was used in this work. It is stated by Eagle Picher to be 99.9999% purity and is -8 +20 mesh, product code UHP6-4003, with a date of manufacture 12/98. The certificate of analysis lists the elements Ag, Al, As, Ba, Bi, Cd, Co, Cr, Cu, Ga, Ge, Hg, K, Li, Mg, Mn, Na, Ni, P, Pb, Sb, Se, Si, Sn, Sr, and Zn in amounts less than 0.1 ppm, Ca < 0.5 ppm, and Fe = 0.12 ppm. The stated overall purity does not reflect the carbon content of the boron, which is typically in the range from 20-50 ppm.

Weighed amounts of the powder were placed on a water-cooled copper hearth and melted to form dense samples of approximately 3 mm diameter for use in the levitation melting and purification by reaction with oxygen. The first method for fusing the powder used arc melting, but this technique presents the potential for contamination with tungsten from the arc electrode. Therefore, the method was changed, to employ CO_2 laser beam melting on a copper hearth, under a high purity argon atmosphere. Previous research has demonstrated undetectable copper contamination of oxide materials that are laser melted on a copper hearth. At the melting point of boron, the vapor pressure of copper is approximately 5000 times that of boron, sufficient that any slight contamination by copper during sample preparation will be removed in a few seconds, by vaporization in the subsequent containerless processing experiment.

The purification process was to first levitate a boron sample in a conical nozzle levitation device, in which CO_2 laser beam heating is used to melt the levitated material. Approximately 100 watts of CO_2 laser beam power is required to heat a 3 mm sample to the melting point (melting temperature = 2360K), and a power increase to approximately 250 watts is required to completely melt the levitated sample. Larger specimens could not be completely melted.

The molten samples were purified by reaction with a controlled flow of 1% O_2 in Ar gas that was added to the pure Ar gas in which the sample was first levitated. Total O_2 flow rate was 0.1 to 0.4 sccm. In 15-minute test experiments, the mass loss varied linearly with the oxygen flow up to 9% loss from a 33 mg boron sample with 0.4 sccm O_2. The mass loss indicates that more than 50% of the oxygen reacts with the sample to form gaseous BO and CO products. Based on these results, the protocol chosen for purification of samples was to levitate, melt, and react with oxygen under conditions that will yield a total sample mass loss of approximately 5%. The oxygen flow was turned on after stable levitation of the liquid was achieved. After a timed

interval, the oxygen was turned off and the sample held near the melting point for a few minutes, before cooling to room temperature by turning off the laser beam heating.

2.2.1 Hearth-Melting Experiments

Hearth melting experiments were performed on boron samples of different size to investigate the relationship between the sample size and heating conditions. It was found that 3 mm diameter specimens can be fully melted on the water cooled copper hearth with a maximum CO_2 laser heating power of approximately 250 watts. Larger samples formed by partial melting of several 3 mm samples together could not be completely melted.

2.2.2 Observations on Laser-Heated Boron

Figure 4 illustrates the video image of a partially molten sample of approximately 5.8 mm diameter, heated with 250 watts of laser heating power. The video image, obtained through the pyrometer, shows a central molten region of the sample that is surrounded by a thin band of solid boron at the melting point. There is good contrast at the interface between solid and liquid, due to a smaller value for the spectral emissivity of the liquid, 0.31, than for the solid, 0.68. The viewing angle for the video was approximately 45° from vertical so that the bright heated region has an oval shape in the image.

Figure 5 illustrates the surface temperature gradients that were measured over the surface of the sample illustrated in Figure 4. The three curves in Figure 5 correspond to different focussing conditions for the heating laser beam. The liquid region extends from approximately -2 mm to +2.5 mm on the horizontal axis. The increased apparent temperature of the solid at the solid liquid interface is not resolved because of the finite spot size of the pyrometer detector. (The circle within cross hairs shown in Figure 4 is the approximate region resolved by the pyrometer.)

The temperatures shown in Figure 5 may be evaluated by comparison with the apparent temperatures at the melting point that are determined from known emissivities for the solid and liquid. The measured temperatures are also reduced by non-unit transmission by the pyrometer window and close-up lenses used on the pyrometer. There were two close-up lenses and the window, each with a transmission of approximately 0.92. The (normal spectral) emissivities at the pyrometer wavelength (0.65 μm) for liquid and solid boron at the melting point are 0.31 and 0.68, respectively. The melting point is 2360K, which gives the following apparent temperatures that would apply in the experiment:

Apparent melting temperature of liquid boron at 2360K:	2049K	1776°C
Apparent melting temperature of solid boron at 2360K:	2210K	1937°C

The maximum in apparent temperature at the center of the liquid region is 1895°C, which yields a true temperature for the liquid equal to 2518K, 158K above the melting point of boron. This degree of superheating would have useful application in the boron source, since the flux of boron at 2519K is approximately 5 times larger than at the melting point. If the entire top surface of a 6 mm liquid region can be heated to this temperature, the pH_2/boron deposition rate can be

increased to 5 times the values given in the first row of Table 1.

The apparent temperature near the solid/liquid boundary, as shown in Figure 5, is in the range 1810-1850°C. It is in the expected range that can be resolved by the pyrometer, between the apparent temperature values for the solid and liquid at the melting point of boron.

2.3 Deposition Rate Experiments

The deposition experiments were performed in a vacuum, and the vapor flux was created by heating and melting the surface of high-purity boron specimens of varying size and shape with the CO_2 laser beam. The deposition rate monitor, located 22.7 cm from the samples, made its measurements based upon changes in oscillation frequency of a quartz crystal sensor. The deposition monitor responds to changes in temperature as well as the deposited mass. A temperature-controlled flow of cooling water was delivered to the cooling system of the monitor to help control the crystal oscillator temperature. Initial and final mass measurements of the boron specimens were taken during preliminary experimentation, and the sample mass and approximate sample diameters were recorded. Three different types of boron samples were used, as described below and illustrated in Figure 6.

1. Spherical samples, which were levitated and purified using a CO_2 laser. The samples were 33 +/- 5 mg mass, and ≈ 3 mm diameter.

2. Laser-welded samples, typically asymmetrical and rough-surfaced, made of 3 or more spherical samples. The samples were 70-115 mg mass and ≈ 5 mm diameter.

3. Arc-melted samples, half-spheres with a flattened top. The samples were 150-250 mg mass and ≈ 6 mm diameter.

Unless specified, experiments were performed at or below a pressure of $7x10^{-6}$ Torr. Throughout experimentation, the lens that focuses the laser beam was adjusted, and laser power was often varied as well. A computer program was used to record the total deposition in Å, the deposition rate in Å/s, and the apparent temperature of the boron specimen as measured by the spectral radiation pyrometer.

2.4 General Observations

Upon initial heating, boron specimens began to glow red at about 25% output from the 250 Watt CO_2 laser. A viewing shield was needed to observe the sample through the observation window, due to the high intensity of light from the sample. At 40% power, a dark red spot appeared through the viewing shield where the beam was most intense and liquid first formed. The area of liquid phase increased and was a maximum at approximately 75% power output from the laser, see Figure 7. The maximum area of liquid was approximately 2 mm diameter on the 3 mm samples and it increased to nearly 3 mm on the larger, laser welded or arc melted samples.

An increase in deposition rate accompanied the increase in liquid boron area. Apparent temperature at the center of the liquid region was approximately 2000 K, decreasing slightly

with time. In experiments of 10-20 minutes duration, a film would begin to deposit on the viewing window and on the pyrometry window if the pyrometer window shutter was open. As the deposit formed, light transmission by the viewing window decreased and the viewing screen could be removed. The hot sample then appeared white-hot through the boron-coated window.

Slight adjustments of the laser beam position on the sample had a temporary effect on deposition rate, increasing the rate for a few seconds. Chamber pressure increased upon initial sample heating, then tended to decrease, typically about 3 μ-Torr, during experiments. When the chamber was let up to argon after an experiment, deposition readouts on the monitor could increase 100 Å or more. This was generally followed by a decrease in the readout to the original value when the chamber was pumped down again. When the viewing window was removed for cleaning, the deposit on it appeared opaque or translucent. The side that faced the sample had a metallic blue appearance and the interface with the pyrex window was silvery and reflective. The window deposits did not occur during boron melting experiments at a chamber pressure of 1 Torr. Sometimes, burn marks appeared on the Pyrex window, evidently due to intense reflection and perhaps focussing of the laser beam at curved portions of the sample surface. When this occurred, the chamber near the viewing window would usually become too hot to touch.

After each experiment, the observation window was removed and cleaned with nitric acid, water, and alcohol. The boron sample was weighed. The region of the boron samples that was melted had a smooth and silvery appearance after cooling, and showed a small indentation where the laser had been focused, see Figure 8.

2.5 Preliminary Results

Preliminary experiments were used to develop protocols for operating the apparatus. Slight modifications of the apparatus were made during these experiments.

1. Slight heating of the deposition monitor resulted in a negative excursion in the output reading from the monitor when laser heating of the sample was turned on or the deposition shutter was opened. Since only positive readings were recorded by the system, it was necessary to begin experiments without zeroing the deposition monitor, so that the rate of deposition immediately following the initial heating effect would be recorded.

2. The deposition monitor responded to the total mass deposited on the quartz crystal. Its output was in Å/s, as determined by the density of the deposit that was programmed into the device. A density of 2.54 g/cm^3 was used, which is the conversion factor for recovering the integrated mass flux from the thickness output.

3. Various experiments were performed to assess the relationship between the mass deposition rate and laser heating conditions, appearance of the sample as viewed with the video camera, and sample temperature.

4. In one experiment, a Pyrex window was used to block CO_2 laser radiation that was reflected onto the deposition monitor. The pressure in the chamber was set to ~ 1 Torr to

prevent vapor deposition on the pyrex window This experiment separated the effects on the response of the deposition monitor of reflected CO_2 laser energy and radiant energy emitted by the boron sample.

5. It was recognized that light reflected from surfaces could increase the effect of radiant heating on the output of the deposition monitor. Baffles were added in the tube connecting the heating chamber to the deposition monitor to reduce the heating effects.

2.6 Deposition Rate Measurements

Figure 9 illustrates the effect of baffles on reducing radiant heating of the deposition monitor. The panel on the left side (9a) shows results of an early experiment without baffles, which explored effects of opening and closing the shutter on the deposition monitor, moving the laser beam heating position on the sample, and turning laser heating off with the deposition monitor shutter open. The right hand panel (9b) shows results of a later experiment with three baffles to reduce the reflection of radiant heat or laser radiation onto the deposition monitor. In both experiments, a large boron sample was used and the surface was tilted 45° to vertical and perpendicular to the direction of the deposition monitor. The baffles are seen to reduce the effect of opening and closing the shutter on the readout of the deposition monitor. With baffles, this excursion was decreased by a factor of approximately 2.7.

Figure 10 isolates the effects on the readout of the deposition monitor of (i) reflected CO_2 laser energy and (ii) radiant heat from the sample. In these experiments, the apparatus was operated under a 1.2 Torr pressure of Ar to prevent boron vapor from depositing on the deposition monitor. Both panels of the figure show the excursions in readout of the deposition monitor when the shutter was opened and closed, exposing the monitor to the heating radiation. The left hand panel (10a) records total heating effect from CO_2 laser energy and radiant emission from the sample. The CO_2 laser energy was blocked by a pyrex window for the experiment shown in the right hand panel (10b) of the figure, and the excursion due to heating is seen to be reduced. These results show that the effects of reflected CO_2 energy and radiant emission from the sample are approximately equal. Some further improvements in trapping the reflected CO_2 energy can be made. Thus, the reflection of laser heating energy to the deposition monitor or to the cryostat in HEDM experiments will be a minor effect compared to radiant heating by emission from the specimen.

The deposition rate was measured as a function of the laser power output. A small rate was observed at 25% output power, which increased with increasing laser power up to 50%, as liquid formed on the boron sample surface. After the sample surface was melted, the deposition rate became nearly independent of laser power.

Figure 11 illustrates the results from Expt. E24-B, a longer-term experiment in which the boron deposition rate was measured over a 100 minute period. An arc-melted boron sample was used for this experiment and it was tilted so that the heated surface faced the deposition monitor. Adjustments to the NaCl shield and slight adjustments to the heating laser beam position were made during the experiment. In this and all other experiments, the rate measurements were recorded by measuring the voltage output of the deposition monitor, and calibrating these

measurements against the numerical values shown on the monitor panel. The voltage resets to zero after a cumulative output of approximately 820 Å. This was the only experiment that encountered the limit, and slight non-linearity in output was observed near the maximum voltage. A highly linear increase with time in the total deposit thickness is demonstrated by the result, although the measured rate was reduced slightly after re-zeroing the voltage output. For the first hour, the deposition rate was constant, and equal to 0.138 Å/s.

Details from a number of experiments are summarized in Table 2. Some of these experiments were performed in successive runs on a loosely packed pile of high purity boron powder, as indicated by the sample designator. The initial and final mass and mass loss are given in the table. Variables include the chiller temperature that controlled the deposition monitor temperature, the laser power, and CO_2 laser focusing lens position.

Table 2 Summary Results of Boron Vaporization Experiments

Sample	Mass (mg)*			Chiller	Power	Lens	Rate
	Initial	Final	Loss	Temp, C	Watts	pos. cm	Å/s
E5	28.46	23.98	4..48	35.2	120		0.090
E9	95.60	90.62	4.98	35.6	225	10	0.118
E10	37.86	33.32	4.54	19.9	150-250	10	0.078
E12	32.08	28.01	4.07	19.9	100-175	6.7	0.087
E15-2	75.63	72.15	3.48	19.9	250	8.5	0.104
Pile A	101.56	97.56	4.*	19.9	250	7.25	0.088
Pile B	97.56	93.56	4.*	19.9	250	7.75	0.108
Pile C	93.56	89.56	4.*	19.9	250	8.6	0.089
Pile D	89.56	85.56	4.*	19.9	250	8.6	0.084
E16-A	242.59	239.29	33.0	19.9	250	8.3	0.109
E16-B	239.29	236.47	2.82	19.9	250	8.3	0.104
E24-B#	181.36	161.74	19.62	19.9	250	8.3	0.138

* Mass loss was estimated.

Sample inclined towards deposition monitor.

The rate of deposition determined from the thickness *versus* time recorded by the deposition monitor is shown *versus* sample mass in Figure 12. It is seen that the rate of deposition increased with sample mass up to approximately 0.1 gram mass.

2.6.1 Discussion of the Deposition Rate Results

The rates of deposition are calculated from the vapor pressure of boron in Table 3, for vapor

source areas of 2-4 mm diameter, and for temperatures at the melting point and 50K above the melting point.

Table 3 Predicted Rates of Deposition at 22.7 cm from the Boron Vapor Source

Temperature K	Boron Source Conditions			Deposition rate, Å/s	
	P, Torr	Equilibrium flux, $cm^{-2}s^{-1}$	Source diam., mm	Horizontal sample	Inclined sample
2360	9.88×10^{-3}	2.17×10^{18}	2	0.021	0.030
			3	0.047	0.067
			4	0.084	0.119
2410	1.73×10^{-2}	3.77×10^{18}	2	0.037	0.052
			3	0.082	0.116
			4	0.146	0.207

The measured rates are consistent with rates for an evaporating area of 2-3 mm for the smaller 3 mm diameter samples, and 3-4 mm for the larger samples, in agreement with the observed liquid diameter of approximately 2 mm for smaller samples and 3 mm for larger samples.

2.7 Boron Deposition Efficiency

The efficiency of boron collection by the deposition monitor is analyzed in Table 4. The table reports four experiments performed on samples with nominally horizontal evaporating surfaces and the result from Expt. E24-B with sample tilted towards the boron monitor. The initial mass and mass loss, Δm, are shown for the experiments, along with the thickness, t, of the deposit collected by the deposition monitor. The thickness values shown equal the difference between the final and initial readings of the deposition monitor, plus added amounts for periods during the experiments when the deposition monitor was shuttered. The last two columns report the thickness of deposit collected for a given amount of mass evaporated, and the deposition efficiency. The efficiency is taken equal to the ratio of $t/\Delta m$ to the value of this quantity calculated for diffuse free evaporation of the boron.

Values of $t/\Delta m$ for diffuse free evaporation are not shown in the table. They were calculated as follows. According to the cosine law, diffuse free evaporation from the boron sample will lead to a uniform flux on the surface of a sphere that is tangent to the sample surface. The geometry is illustrated for flat and inclined sample surfaces in Figure 13, with the sphere of uniform flux drawn to pass through the deposition monitor. For each case, the fraction of evaporated boron that reaches the deposition monitor equals the fraction of the sphere surface that the monitor intercepts, in a direction along the sample-to-target axis.

Table 4 Boron Deposition Efficiency

Expt.	Sample Surface	Sample mass, mg	Δm, mg	T, Å	t/Δ m Å/mg	Efficiency
E5	Horizontal	28.46	4.48	119	26.6	1.55
E9	Horizontal	95.6	4.98	141	28.3	1.65
E10	Horizontal	37.96	4.64	99	21.3	1.24
E15-B	Horizontal	75.63	3.48	95	27.3	1.59
E24-B	Inclined	181.36	19.62	748	38.1	1.57

The figure illustrates that, with the inclined boron sample, the sphere area is halved, so that the flux at the deposition monitor is doubled for a given evaporation rate. The projected area of the deposition monitor on the sphere surface decreases by a factor of $2^{1/2}$ for the inclined boron sample. The net result is that the fraction of the boron that evaporates and is collected by the deposition monitor should increase by a factor of $2^{1/2}$ when the sample is inclined towards the deposition monitor.

For the inclined sample, the diameter of the sphere of uniform flux is 22.7 cm and its area is 1,619 cm^2. Evaporation of 1 gram of boron will thus yield a deposit of 1 g/1,619 cm^2 at the deposition monitor. Dividing this quantity by the boron density for which the monitor was calibrated, 2.54 g/cm^3, one obtains a deposit thickness equal to 24,300 Å. Thus, diffuse free evaporation at the boron surface yields a maximum deposition efficiency for the present experiments equal to 24.3 Å/mg for the inclined boron surface, and 17.2 Å/mg for a nominally horizontal boron surface.

2.7.1 Discussion of Deposition Efficiency

The deposition efficiency for the inclined sample in Table 4 is 1.47 times greater than the average value for the nominally horizontal samples. This result is within 4% of the expected factor of $2^{1/2}$ difference between the two sample orientations. However, the measured deposition efficiencies average 50% greater than the values predicted for diffuse free evaporation of boron.

Five mechanisms by which the deposition efficiency may differ from the calculated value for diffuse free evaporation were considered and are discussed below. Two phenomena appear to be responsible for the deposition efficiency values in excess of unity. The first is that the evaporation process is diffuse, but not entirely free. The “blast shield” that surrounds the boron sample reflects boron atoms back onto the evaporating sample and may also reflect boron atoms to the deposition monitor. Thus, the blast shield reduces the mass loss of the boron sample, and can increase the deposition flux. The second is that deposited boron may react with residual gases to produce a deposited mass that exceeds the mass of boron collected.

The five mechanisms considered are:

1. Boron atoms may be reflected onto the deposition monitor from the walls of the apparatus. This effect would increase the deposition efficiency.

2. Some of the boron atoms incident on the deposition monitor may be reflected. This effect would make the deposition efficiency smaller than the predicted value.

3. Boron may be gasified by reaction with residual gas to form gaseous species, e.g., BO(g) that are heavier than boron atoms. Deposition of these gaseous species on the monitor would produce a larger signal than is calculated from the boron mass loss.

4. The mass collected by the deposition monitor may exceed that of the boron atoms *via* gettering of residual gases by the deposited boron. This effect would increase the deposition efficiency.

5. Boron atoms may be reflected from the blast shield that surrounds the boron source and be returned to the boron sample. This effect would decrease the amount of boron that evaporates, and increase the deposition efficiency. It may increase the boron flux at the deposition monitor.

Mechanisms (1) and (2) involve reflection of boron atoms from a boron-covered ambient temperature surface. There is a precedent for the absence of such reflection in the literature. Robson and Gilles [1] measured the vapor pressure of boron carbide contained in carbon effusion cells by a target collection technique, in which such reflection could occur. Their results were in close agreement with the vapor pressure measurements of Hildenbrand and Hall [2] obtained by the torsion effusion method. This agreement shows that reflection from the ambient temperature targets was not a significant process in the vapor pressure measurements. The accuracy of these investigations was uncertain for a long time due to the difficulties in direct measurement of the vapor pressure of boron. It was ultimately confirmed that the earlier results are correct when the enthalpy of formation of boron carbide was reliably measured by high temperature solution calorimetry [3] and the vapor pressure of pure boron [4] was determined by a containerless method that eliminated the reaction of boron with container materials.

An experimental check was performed on the reflection of boron atoms from ambient temperature boron-coated surfaces. A funnel-shaped steel tube was placed in the arm of the apparatus leading to the deposition monitor, and designed to reflect boron atoms onto the deposition sensor. A beam block was placed in the path to eliminate direct deposition of atoms from the boron source without restricting the boron flux onto the funnel surface. No detectable deposition of boron atoms occurred, showing insignificant reflection of boron atoms at the funnel surface. The experiment showed that reflection of boron atoms does not occur at ambient temperature boron covered surfaces such as the apparatus walls and sensor surface.

Mechanism (3) is demonstrably negligible. The vapor pressure of boron at the melting point is

9.88×10^{-3} Torr, while the residual gas pressure in the system was approximately 10^{-6} Torr. Therefore, the flux of gasified species must be negligible compared with that of atomic boron.

By mass balance, mechanism (4) can contribute to the deposition mass flux if a sufficient fraction of incident gas molecules react with boron to form a condensed reaction product. The typical deposition rate of 0.1 Å/s is equivalent to a boron flux of 2.54×10^{-9} g/cm^2 s, while, at 10^{-6} Torr of air, the incident O_2 flux (4.0×10^{-9} g/cm^2 s) and N_2 flux (1.4×10^{-8} g/cm^2 s) can contribute a substantial additional reactive mass flux. For example, the mass deposited would be 50% greater than the mass of boron if reaction with ambient oxygen or nitrogen formed a condensed product whose composition is $BO_{0.34}$ or $BN_{0.39}$.

Consider, however, the pumping rate for residual gas that is implied by the mass balance. The boron evaporation rate is approximately 4×10^{-6} g/s. The residual gas pressure in the system was 1×10^{-6} to 7×10^{-6} Torr and the turbomolecular pumping speed was 40 liter/s. At these pressures, the turbomolecular pump removes 6.2×10^{-8} to 4.3×10^{-7} g/s of residual gas. This is the supply of air available for reaction with boron, and equals only 1.6 to 11% of the boron evaporation rate, depending on pressure. Thus, there was an insufficient residual gas supply to explain the 50% excess in deposition rate over the value calculated for diffuse free evaporation of boron. Therefore, reaction with residual gas by mechanism (4) could explain a minor part, but not all, of the departure from unit deposition efficiency.

Mechanism (5), reflection from the blast shield, was demonstrated by the deposition of boron on chamber walls where boron could not deposit by free evaporation from the boron surface. This result is consistent with the less than unity evaporation coefficient of solid boron, which is approximately 0.3, i.e., free evaporation of solid boron [5] occurs at 30% of the boron flux in saturated vapor. The reflection coefficient is thus equal to approximately 0.7 at a temperature near the melting point and it may be quite large on the blast shield which is heated to a temperature near 1000K by reflected laser radiation.

Approximately 20% of the blast shield area is open, for observation, laser heating, and transmission of vapor to the deposition monitor and the boron samples comprised less than 5% of the area enclosed by the blast shield. It was estimated that reflection at the blast shield can explain part, but not all of the departure from unit deposition efficiency.

3.0 CONCLUSIONS

The overall objective of this research was met by demonstrating a practical source of boron vapor that can be used for R&D on B/pH_2 HEDM.

1. Reproducible boron vapor fluxes were obtained, in part through the intrinsic temperature control at the melting point of boron that is achieved by the CO_2 laser beam-heating method. Reflection of CO_2 laser radiation increases upon melting to yield a liquid vapor source whose temperature remains within about 50K of the melting point. A stable flux of boron atoms is thus obtained for controlled doping of the pH_2 with a uniform-concentration of boron atoms for HEDM applications.

2. The measured boron fluxes agree well with the fluxes predicted for diffuse free evaporation from the vapor source. The estimated distance to the deposition region for HEDM application is approximately 10 cm. At this distance, the deposited flux of boron atoms would be approximately 0.72 Å/s, equivalent to 1.8×10^{-8} g/cm^2 s or 6.1×10^{-6} mole/cm^2-hour of boron. At this boron flux, the HEDM deposition rates given in Table 5 would be possible.

Table 5 Estimated Maximum Deposition Rates for Boron-Doped pH_2 HEDM

Boron concentration	HEDM deposition rate
0.1 mol %	1400 μm/hour
1 mol %	140 μm/hour
5 mol %	28 μm/hour

3. The intensity of CO_2 laser beam heating radiation that is reflected to the deposition monitor (or to the cryogenic equipment for HEDM studies) can be controlled to be a small fraction of the radiant emission from the boron vapor source. The heat load on cryogenic equipment would then be somewhat less than the blackbody emission from a 2360K source, since the emissivity of boron is less than unity. The deposition rates given above can be achieved at a distance of 10 cm from a boron vapor source of approximately 5 mm diameter. The radiant heat load on the cryogenic equipment is thus estimated to be less than 0.1 watt/cm^2.

4.0 DESIGN FOR PHASE II

The primary objective in Phase II will be to deliver a boron source apparatus to AFRL for use in preparing HEDM materials consisting of boron atom-doped pH_2. The concepts developed for phase II and detailed in the Phase II proposal include:

1. A well controlled and instrumented laser-heated boron vapor source was proposed for use in spectroscopy research on boron-doped pH_2. Since much of the research involves boron concentrations that are significantly less than 1 mol %, the distance between the vapor source and cryogenic equipment may be increased and the boron sample oriented to facilitate integration of a deposition monitor, optical pyrometer, and a gate valve located between the boron source and cryogenic equipment.

2. A minimally-instrumented apparatus was proposed in which the orientation and location of the boron vapor source are designed to maximize the boron flux for preparation of high concentrations of B/pH_2. The intrinsic temperature control at the melting point that is achieved in CO_2 laser heating of boron facilitates this application while allowing a highly predictable control of the boron flux and HEDM concentration.

3. R&D was proposed to investigate the behavior of highly doped B/solid Ar as a prototype for highly doped B/pH_2 HEDM. The study of B/solid Ar would include studies of the optical emission and energy release that occurs when B atoms are allowed to recombine by warming of the cryogenic solid. It will include work on the preparation and storage of relatively large quantities of B-doped solid Ar.

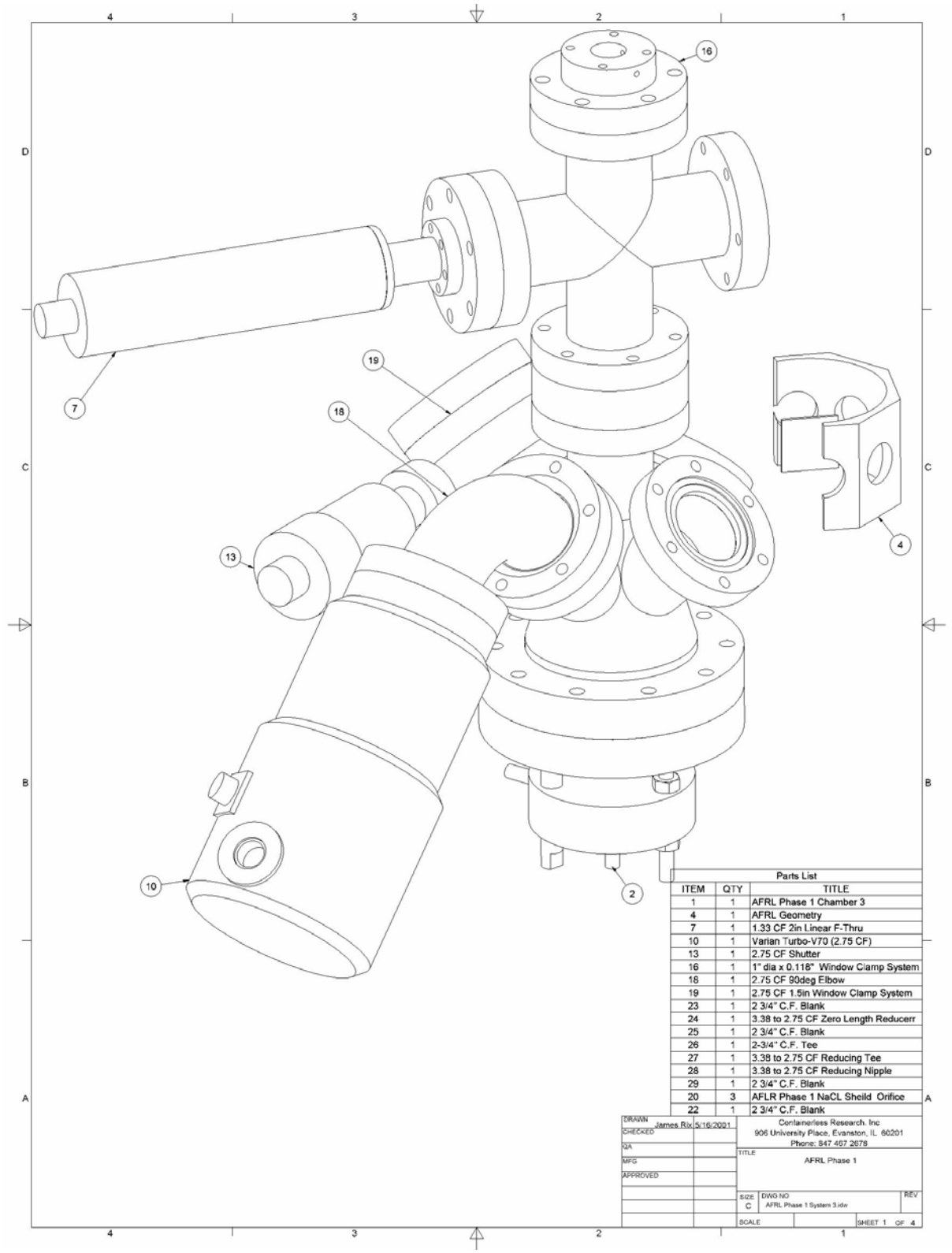

Figure 1 Design of the Boron Vapor Source

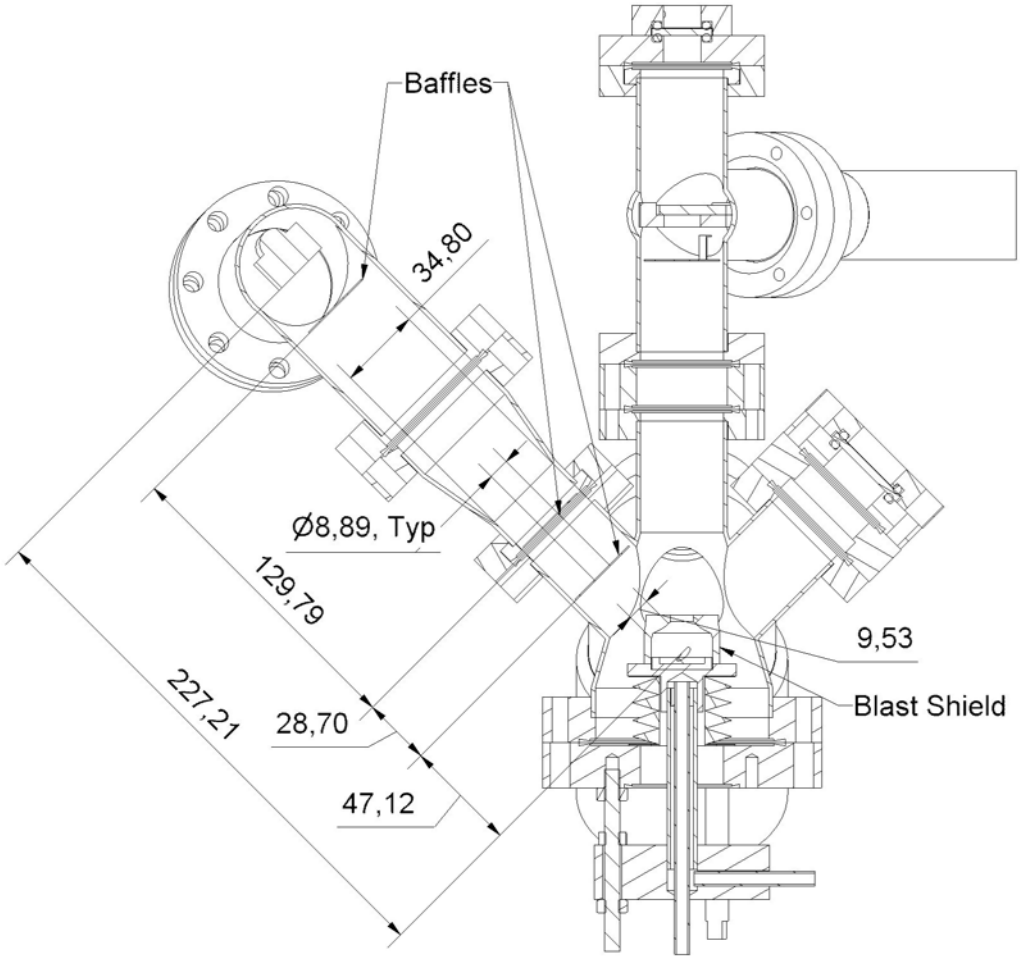

Figure 2 Drawing of the Boron Vapor Source

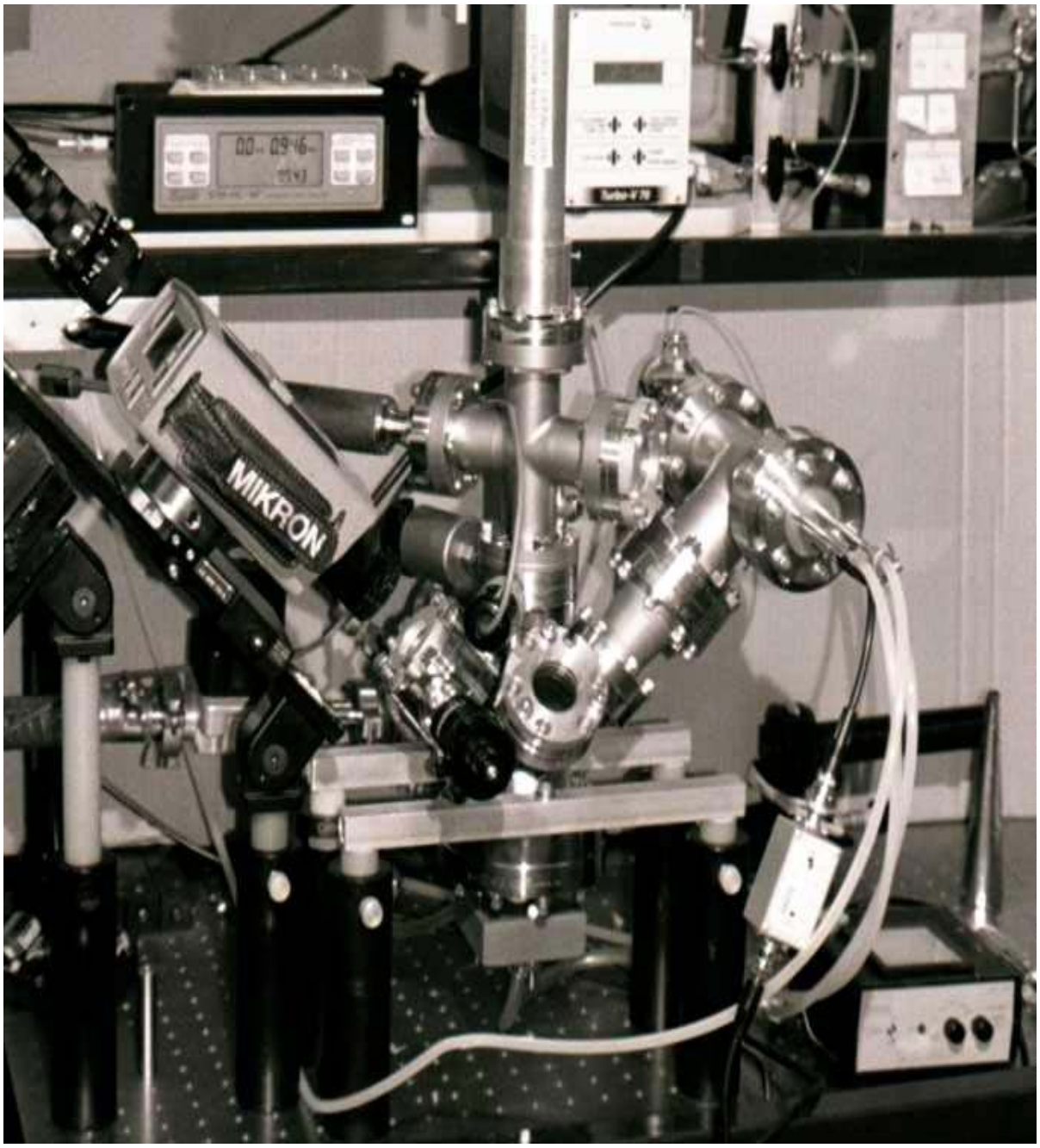

Figure 3 Photograph of the Boron Vapor Source

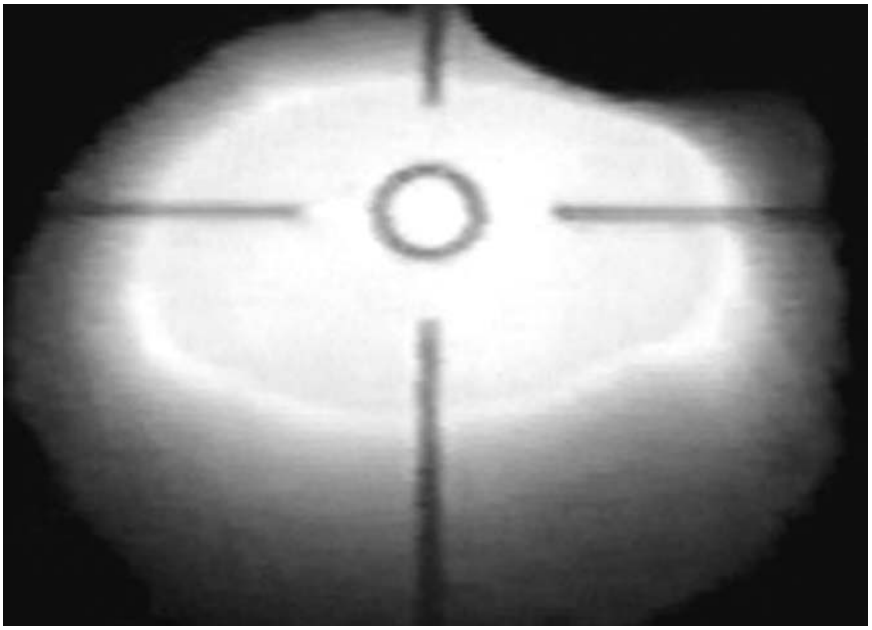

Figure 4 Video Image of a Partially Molten Boron Sample

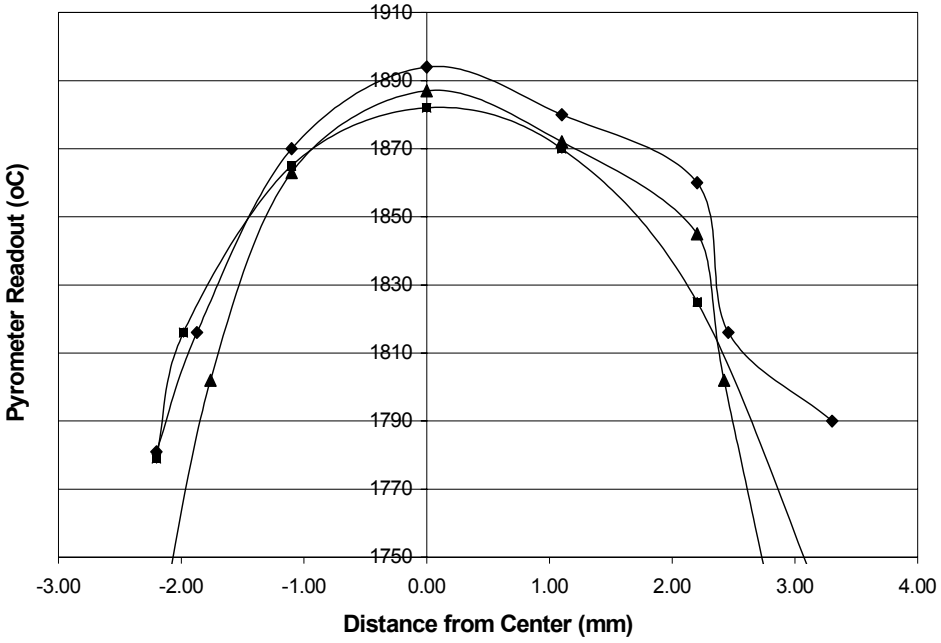

Figure 5 Apparent Temperature Measurements on Hearth-Melted Boron

Sample diameter = 5.8 mm, CO_2 laser heating power = 250 watts

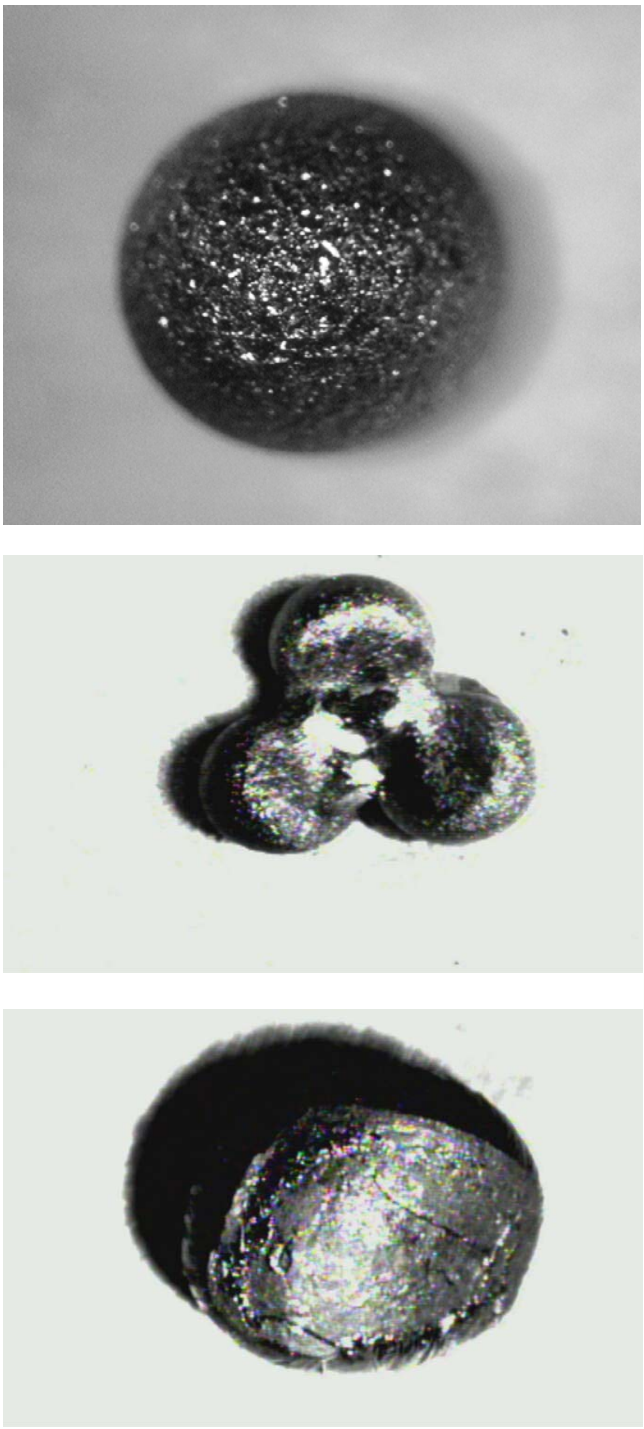

Figure 6 Boron Samples

Top: 3 mm spheroids; middle: laser-welded spheroids; bottom: large, arc-melted sample

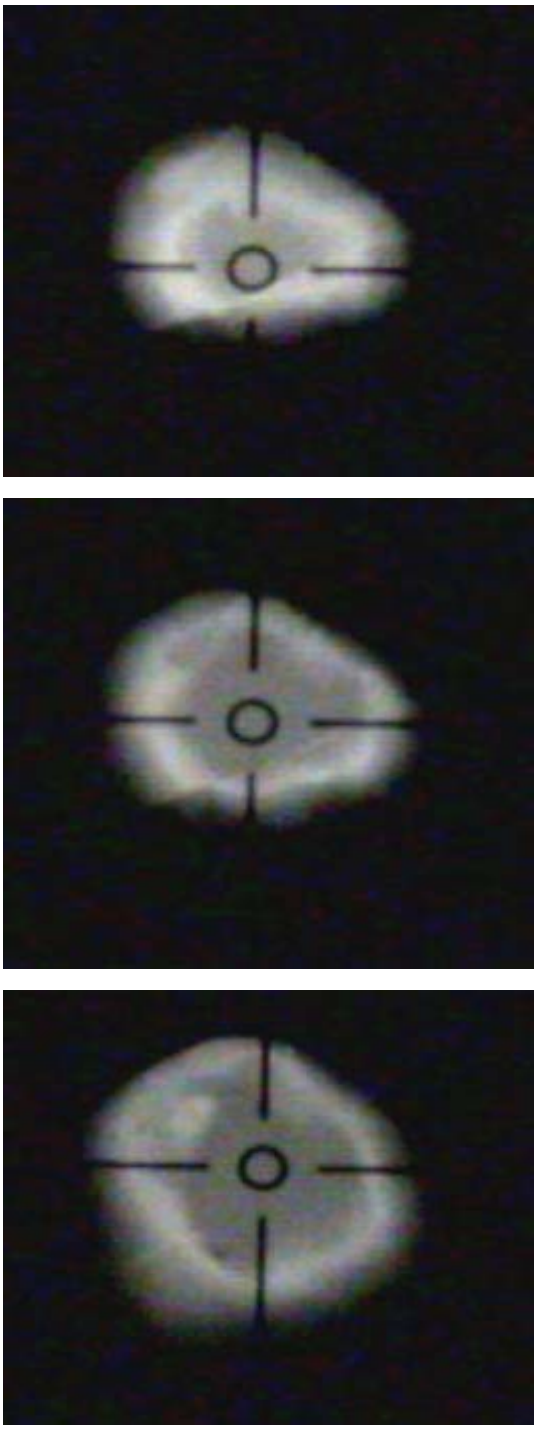

Figure 7 Video Camera Views of Laser Heated Boron

Top-to-bottom: Heated at 25, 50, and 100% laser output power

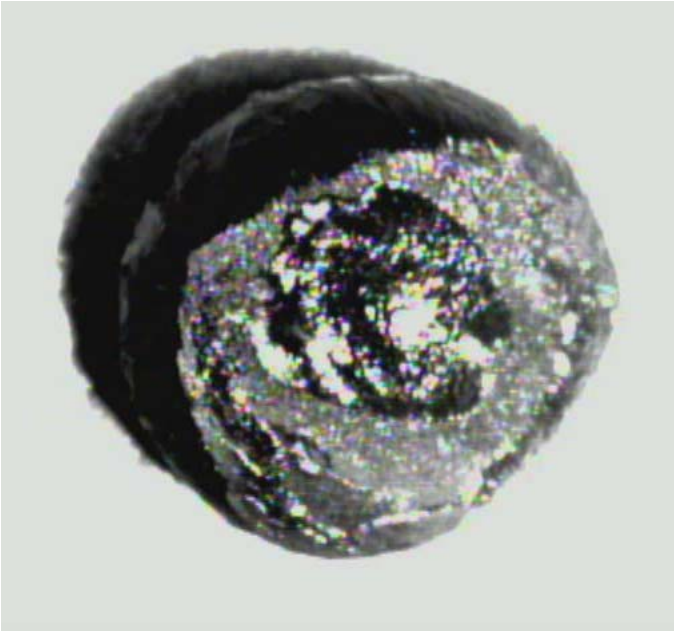

Figure 8 Large, Arc Melted Sample after Laser Heated Vaporization Experiment

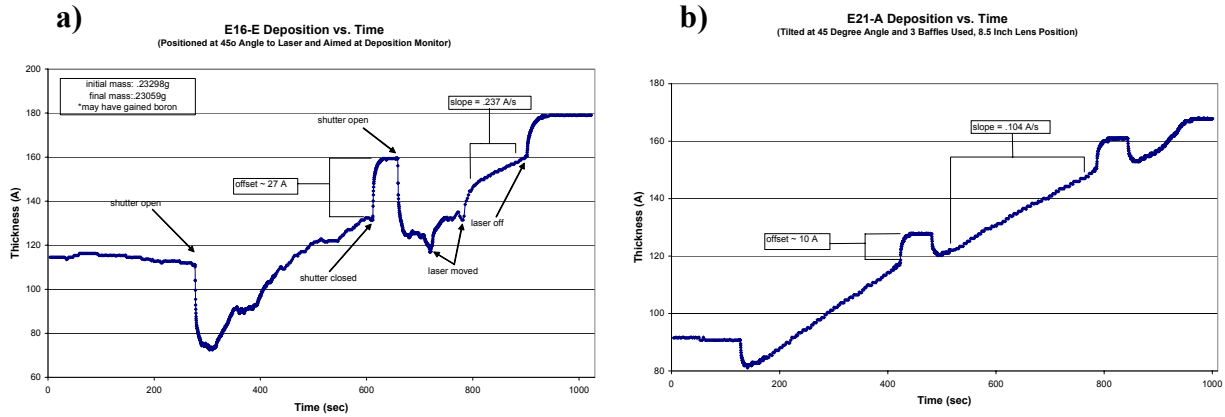

Figure 9 Excursion of the Deposition Monitor Readout due to Heating Effects

(9a) Left - Without Baffles to Limit Heating of the Deposition Monitor

(9b) Right - Reduced Heating Effects with Baffles

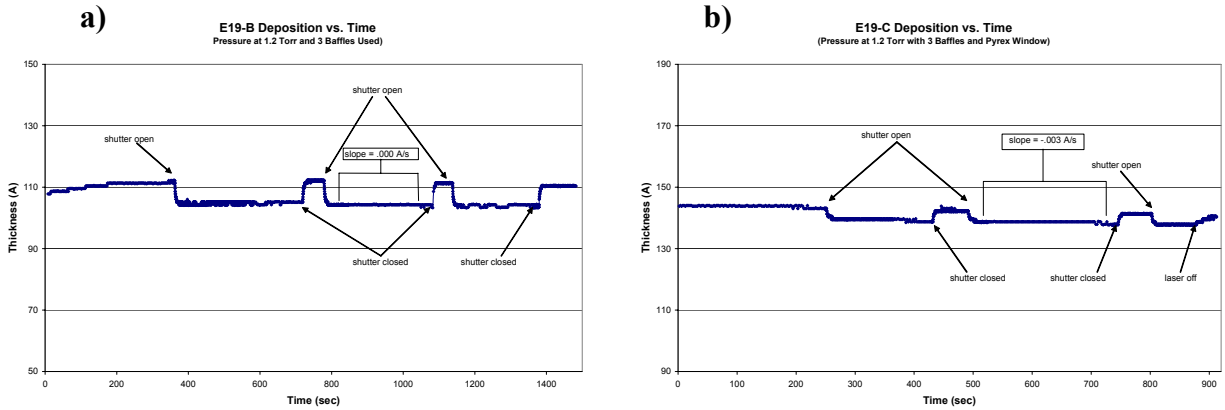

Figure 10 Laser Heating and Radiant Heating of the Deposition Sensor

(10a) Left - Under 1.5 Torr Ar gas

(10b) Right - With a Pyrex Window to Block CO_2 Laser Energy at the Deposition Sensor

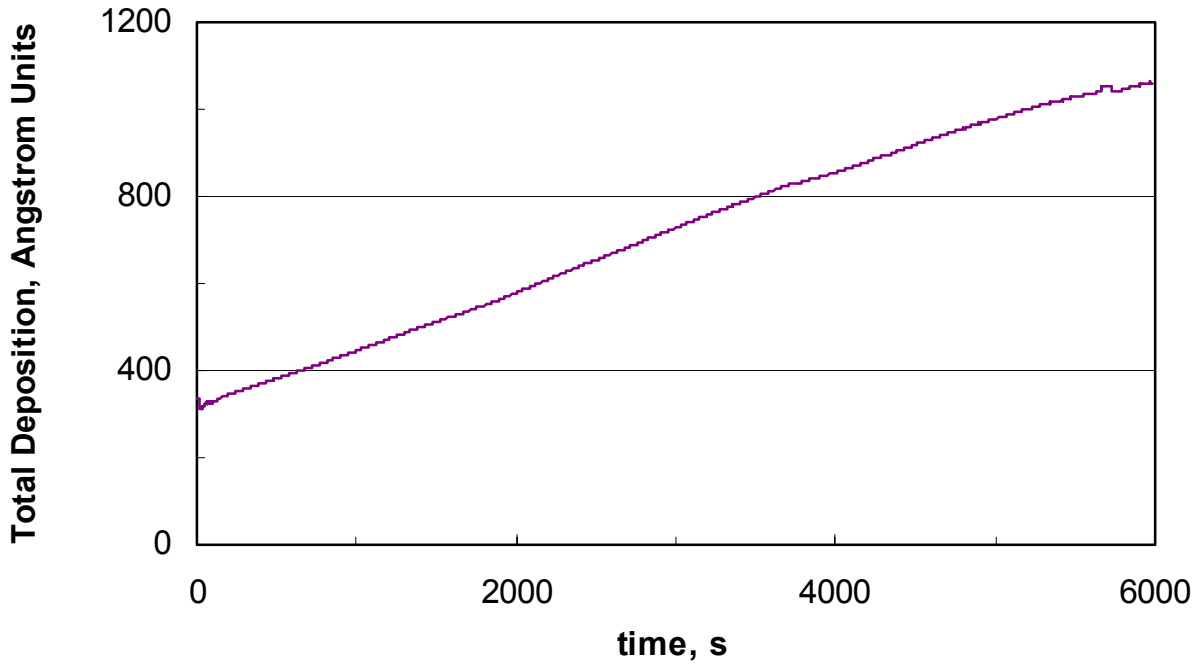

Figure 11 Long-Term Deposition Experiment No. E24-B

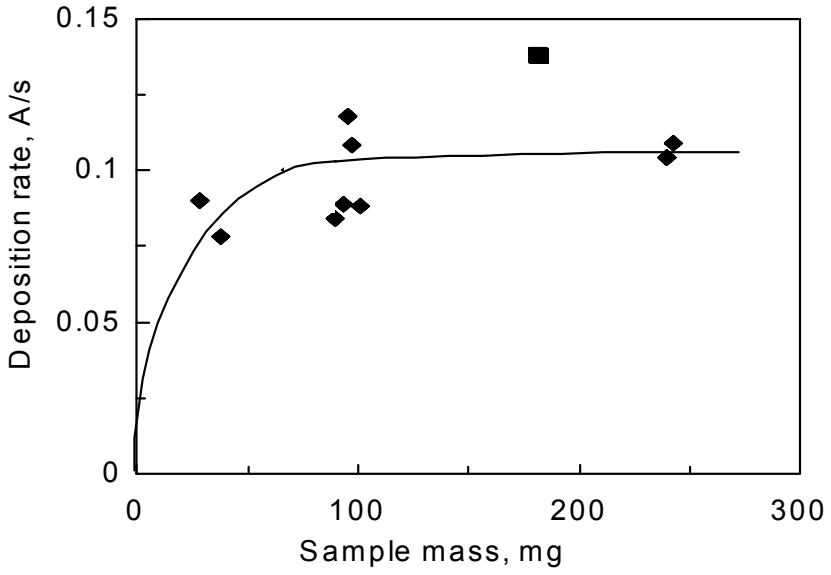

Figure 12 Rate of Deposition *versus* Sample Mass

The solid square is for a sample tilted toward the deposition monitor

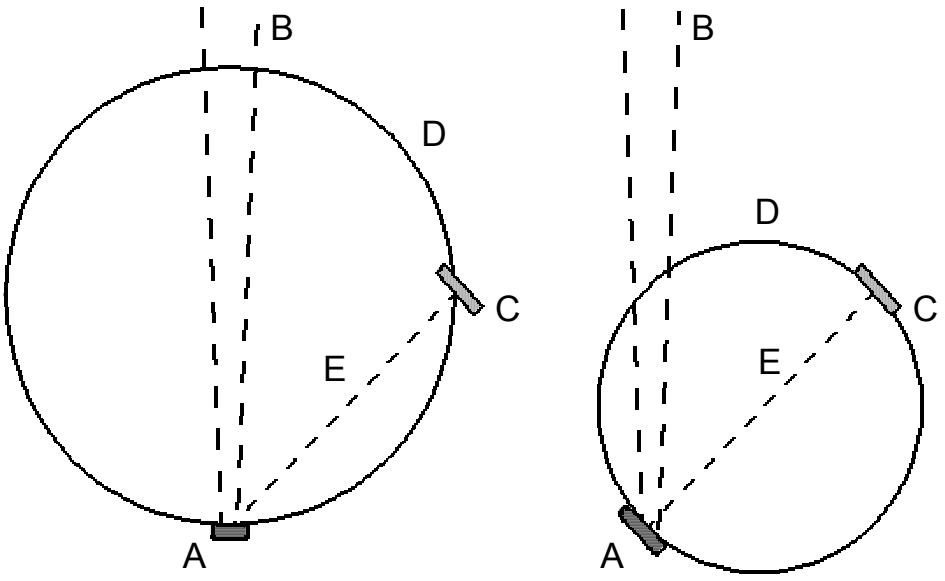

Figure 13 Analysis of Diffuse Evaporation from Horizontal (left) and Inclined (right) Boron Samples

A – Boron Sample; B – CO_2 laser heating beam; C – Deposition sensor; D – sphere of uniform flux; E – Sample-to-target axis

REFERENCES

1. Robson, H.E. and Gilles, P.W., *J. Phys Chem.* **68**, 1964, pp. 983.
2. Hildenbrand, D.L. and Hall, W.F., *J. Phys. Chem.* **68**, 1964, pp. 989.
3. Topor, L. and Kleppa, O.J., *J. Chem Thermodynamics* **16**, 1984, pp. 993.
4. Nordine, P.C., Weber, J.K.R, Krishnan, S., and Schiffman, R.A., *High Temp. Science* **30**, 1991, pp. 163.
5. Paule, R.G. and Margrave, J.L., *J. Phys. Chem.* **67**, 1963, pp. 1369.

This Page Intentionally Left Blank

AFRL-PR-ED-TR-2003-0030
Primary Distribution of this Report:

AFRL/PRSP (10 HC)
Dr. Bill Larson
10 East Saturn Blvd
Edwards AFB CA 93524-7680

Paul C. Nordine (1 HC)
Containerless Research Inc.
906 University Place
Evanston IL 60201-3149

AFRL/PR Technical Library (2 CD + 1 HC)
6 Draco Drive
Edwards AFB CA 93524-7130

Chemical Propulsion Information Agency (1 CD)
Attn: Tech Lib (Dottie Becker)
10630 Little Patuxent Parkway, Suite 202
Columbia MD 21044-3200

Defense Technical Information Center
(1 Electronic Submission via STINT)
Attn: DTIC-ACQS (Acquisitions)
8725 John J. Kingman Road, Suite 94
Ft. Belvoir VA 22060-6218

Deborah A. Spotts (1 CD + 1 HC)
AFRL/PROI (SBIR)
5 Pollux Drive
Edwards AFB CA 93524-7003

Ranney Adams (1 CD + 1 HC)
AFRL/PROI
5 Pollux Drive
Edwards AFB CA 93523-7003